

Development and Validation of NCAR Whole Atmosphere Community Climate Model with Thermosphere/Ionosphere Extension (WACCM-X)

*Hanli Liu¹

1. National Center for Atmospheric Research

The NCAR Whole Atmosphere Community Climate Model with Thermosphere/Ionosphere Extension (WACCM-X) has been developed to study the solar impact on the Earth system, to understand and quantify couplings between atmospheric layers through chemical, physical and dynamical processes, and to investigate the implications of the couplings to climate (downward coupling) and to space environment (upward coupling). This talk discusses recent development of WACCM-X, including newly implemented modules of ionospheric electrodynamics, O⁺ transport and plasma temperatures, as well as modification of model dynamical core for the thermosphere, where mean molecular mass and specific heats are variables. With the interactive ionosphere modules and the improved dycore, we have made extensive simulations to validate the thermosphere and ionosphere results. The thermospheric compositional structure are in good agreement with climatology. Atmospheric tides, which are important in controlling the dynamics, transport and electrodynamics in the upper atmosphere but were underestimated in earlier versions of WACCM-X, are now well resolved and are in good agreement with observations. Ionospheric plasma densities, including the equatorial ionization anomaly (EIA) and zonal and vertical ExB drifts are found to be in good agreement with observations. Variabilities from day-to-day to seasonal scales and solar cycle dependence are also examined.

Keywords: Whole atmosphere model, space weather, lower and upper atmosphere coupling

The Navy Highly Integrated Thermosphere Ionosphere Demonstration System (Navy-HITIDES): Stratospheric Warming, Tides and Annular Modes in a Whole Atmosphere with Ionospheric Effects

*Fabrizio Sassi¹, Sarah E McDonald¹

1. Naval Research Laboratory

We present novel results of a new atmosphere-ionosphere integrated system developed at the Naval Research Laboratory (NRL) that allows the investigation of lower atmospheric effects on the upper mesosphere, lower thermosphere and the ionosphere (UMLT-I). The Navy-HITIDES prototype is flexible enough to couple with any neutral atmosphere model, and for the purpose of this talk we have coupled Navy-HITIDES with the NCAR Whole Atmosphere Community Climate Model, extended version (WACCM-X); the underlying ionospheric model is the NRL SAMI3. We will illustrate the motivation for developing Navy-HITIDES, the engineering that makes this model flexible, portable and accurate. We discuss in detail simulations with Navy-HITIDES where the lower atmospheric meteorology is constrained by the prototype Navy high altitude atmospheric analysis (0-90 km), the advantages of nudging with high altitude analysis, as well as its limitations. Particular attention is devoted to the morphology of the UMLT-I, how it changes with stratospheric warming, resolution of tidal motion and annular modes.

Keywords: thermosphere Ionosphere Coupling, whole atmosphere coupling

Observations of the thermal structure, composition, and energy budget of the mesosphere and thermosphere from 15 years of data from SABER

*Martin G Mlynczak¹, Linda A Hunt², James M Russell³, Thomas Marshall⁴

1. NASA Langley Research Center, 2. Science Systems and Applications, Inc. , 3. Hampton University, 4. GATS, Inc.

The Sounding of the Atmosphere using Broadband Emission Radiometry (SABER) instrument has been observing the thermal structure, chemical composition, and energy budget of the Earth' s mesosphere and thermosphere for over 15 years. The instrument is on the NASA Thermosphere-Ionosphere-Mesosphere-Energetics and Dynamics (TIMED) satellite and continues to operate nominally, routinely collecting over 1500 profiles of limb radiance daily in each of its 10 channels. These measurements produce over 30 unique data products. The length of the SABER dataset continues to enable scientific discovery on topics ranging from solar-terrestrial connections to global change due to carbon dioxide increases. In this talk we will review in particular the influence of solar variability on the energy balance, composition, and thermal structure of the upper atmosphere. A specific focus will be on the current state of the Sun as it progresses towards the next solar minimum, and the corresponding effects seen in Earth' s atmosphere. We also will examine the effects of recent high speed solar wind stream events that are now becoming more common in this phase of solar activity, searching for evidence of previously-observed harmonics of the solar rotation period in the infrared cooling budget of the thermosphere. Prospects and requirements for new observations of the ionosphere-thermosphere-mesosphere will also be presented.

Keywords: Mesosphere-Thermosphere, Solar-Terrestrial Coupling, Global Change

Coupling processes in the upper atmosphere revealed by imaging observation of the ISS-IMAP mission

*齊藤 昭則¹、穂積 裕太¹、坂野井 健²、Perwitasari Septi²、吉川 一朗³、山崎 敦⁴、大塚 雄一⁵

*Akinori Saito¹, Yuta Hozumi¹, Takeshi Sakanoi², Septi Perwitasari², Ichiro Yoshikawa³, Atsushi Yamazaki⁴, Yuichi Otsuka⁵

1. 京都大学大学院理学研究科地球物理学教室、2. 東北大学大学院理学研究科惑星プラズマ・大気研究センター、3. 東京大学、4. 宇宙航空研究開発機構 宇宙科学研究所、5. 名古屋大学宇宙地球環境研究所

1. Department of Geophysics, Graduate School of Science, Kyoto University, 2. Planetary Plasma and Atmospheric Research Center, Graduate School of Science, Tohoku University, 3. The University of Tokyo, 4. Institute of Space and Astronautical Science / Japan Aerospace Exploration Agency, 5. Institute for Space-Earth Environmental Research, Nagoya University

Imaging observation of the ISS-IMAP (Ionosphere, Mesosphere, upper Atmosphere, and Plasmasphere mapping) mission detected the airglow in the mesosphere and the lower thermosphere (MLT), and the ion resonant scattering in the ionosphere from 2012 and 2015. It was installed on the Exposure Facility of Japanese Experiment Module of the International Space Station, EF of ISS-JEM, and consisted of two sets of imagers. Visible-light and infrared spectrum imager (VISI) observed the airglow of 730nm (OH, Alt. 85km), 762nm (O₂, Alt. 95km), and 630nm (O, Alt. 250km) in the MLT region, and Extra ultraviolet imager (EUVI) observed the resonant scattering of 30.4nm (He⁺) and 83.4nm (O⁺) from ion in the Ionosphere. Horizontal two-dimensional imaging of VISI frequently detected concentric wave structures in the mesosphere. The wave features of the concentric wave structures imply the propagation direction and the center of the structure. Using them, some of them can be directly connected with the lower atmospheric phenomena, such as tornado and tropical cyclone. This observation revealed the coupling between the lower and the upper atmospheres with atmospheric gravity waves. On the topside of the ionosphere, EUVI detected the interhemispheric asymmetry of the He⁺ ion distribution. It shows clearly longitudinal variations, and implies that the interhemispheric neutral wind and the configuration of the geomagnetic field affect the transport of He⁺ as the result of the coupling process between the neutral atmosphere and the ionized atmosphere on the bottomside of the ionosphere. Results of the imaging observation of the MLT region and the ionosphere from ISS, and the coupling processes will be discussed in the presentation.

キーワード：熱圏、電離圏、中間圏、大気重力波、大気光、国際宇宙ステーション

Keywords: Thermosphere, Ionosphere, Mesosphere, Atmospheric gravity wave, Airglow, International Space Station

Effects of thermospheric gravity waves on the thermosphere-ionosphere system simulated by high resolution GAIA

*三好 勉信¹、陣 英克²、藤原 均³、品川 裕之²

*Yasunobu Miyoshi¹, Hidekatsu Jin², Hitoshi Fujiwara³, Hiroyuki Shinagawa²

1. 九州大学大学院、2. 情報通信研究機構、3. 成蹊大学

1. Kyushu University, 2. NICT, 3. Seikei University

It has been recognized that short-period fluctuations (0.5 hour- 2 hour) associated with gravity waves play an important role on the thermosphere-ionosphere (TI) system. In order to investigate effects of thermospheric gravity waves on the TI system, we have developed an atmosphere-ionosphere coupled model (GAIA) with high horizontal resolution (about 1.0 degree longitude by 1.0 degree latitude). The GAIA contains the region from the ground surface to the upper thermosphere (about 500km altitude), so that we can simulate excitation of gravity waves in the lower atmosphere and their upward propagation to the thermosphere. Furthermore, the GAIA simulation with higher horizontal resolution (about 0.5 degree longitude by 0.5 degree latitude) is conducted. In this study, we focus our attention on gravity wave activity in the winter thermosphere/ionosphere. Our simulation result indicates that fluctuations with periods (0.5 hour - 2 hour) associated with thermospheric gravity waves are more significant in the winter hemisphere. Fluctuations of electron density in the F-region due to upward propagating gravity waves are also studied.

キーワード：熱圏電離圏結合、大気重力波、上下結合

Keywords: Thermosphere-ionosphere coupling, gravity wave, vertical coupling

Thermospheric nitric oxide response to shock-led storms

*Delores Knipp¹, Daniel Pette², Liam Kilcommons², Tristan Isaacs², Alfredo Cruz², Martin Mlynczak³, Linda Hunt⁴, Cissi Lin⁵

1. University of Colorado Boulder and High Altitude Observatory National Center for Atmospheric Research, Boulder CO, USA, 2. University of Colorado Boulder USA, 3. Science Directorate, NASA Langley Research Center, Hampton, Virginia, USA,, 4. Science Systems and Applications, Inc., Hampton, Virginia, USA, 5. Physics Department, University of Texas at Arlington, Arlington, Texas, USA

We present a multiyear superposed epoch study of the Sounding of the Atmosphere using Broadband Emission Radiometry nitric oxide (NO) emission data. NO is a trace constituent in the thermosphere that acts as cooling agent via infrared (IR) emissions. The NO cooling competes with storm time thermospheric heating resulting in a thermostat effect. Our study of nearly 200 events reveals that shock-led interplanetary coronal mass ejections (ICMEs) are prone to early and excessive thermospheric NO production and IR emissions. Excess NO emissions can arrest thermospheric expansion by cooling the thermosphere during intense storms. The strongest events curtail the interval of neutral density increase and produce a phenomenon known as thermospheric “overcooling.” We use Defense Meteorological Satellite Program particle precipitation data to show that interplanetary shocks and their ICME drivers can more than double the fluxes of precipitating particles that are known to trigger the production of thermospheric NO. Coincident increases in Joule heating likely amplify the effect. In turn, NO emissions are more than double. For some events, there may be an additional factor of early NO production due to solar flares. Perhaps a more potent combination of solar wind events involves a series of ICMEs, especially if the interplanetary path has been “cleared” for the second or subsequent ICME. We discuss the roles and features of shock/sheath structures that allow the thermosphere to temper the effects of extreme storm time energy input. Shock-driven thermospheric NO IR cooling likely plays an important role in satellite drag forecasting challenges during extreme events.

Keywords: Thermospheric nitric oxide, Coronal mass ejections, Shock-led storms

Molecular Ion Up-flows and Hot Oxygen Atoms in Magnetosphere-Ionosphere-Thermosphere Coupling

*Andrew W Yau¹, Victoria Foss¹, Bernard D. Shizgal²

1. University of Calgary, 2. University of British Columbia

The CASSIOPE Enhanced Polar Outflow Probe (e-POP) has been in operation since its launch into a polar orbit in September 2013. In the present study, we use the high-resolution in-situ data from e-POP to investigate a specific magnetosphere-ionosphere-thermosphere (MIC) coupling process: the acceleration and up-flows of molecular ions in the auroral ionosphere and the subsequent production of hot neutral oxygen atoms. Specifically, we present observations of enhanced molecular NO^+ and possibly O_2^+ ion densities in the F-region and topside ionosphere (up to ~1000 km altitude), and density and temperature estimates of the hot oxygen atoms resulting from the dissociative recombination of the observed ions: we obtain these estimates by solving the Boltzmann equation for the collisional relaxation between the non-thermal nascent and ambient oxygen atoms, and compare them with previous observations and theoretical model predictions

Keywords: magnetosphere, ionosphere, thermosphere, molecular ions, oxygen

What Drives the Variability of the Mid-Latitude Ionosphere?

*Larisa Goncharenko¹, Shunrong Zhang¹, Philip Erickson¹, V. Lynn Harvey²

1. Massachusetts Institute of Technology Haystack Observatory, USA, 2. Laboratory for Atmospheric and Space Physics, University of Colorado, USA

The superposition of processes driving the short-term variability of ionosphere on scales from several minutes to several days remains one of the challenging topics in ionospheric research. In this study, we aim to 1) quantitatively describe short-term variability in the mid-latitude ionosphere and 2) investigate drivers of this variability. We use over 40 years of observations by the Millstone Hill incoherent scatter radar (42.6°N, 288.5°E) to develop updated empirical model of ionospheric parameters, and wintertime data collected in 2004-2017 to study variability in ionospheric parameters, focusing on ion temperature and electron density. We also use NASA MERRA2 atmospheric reanalysis data to examine possible connections between the state of the stratosphere & mesosphere and the upper atmosphere and ionosphere. Our analysis indicates that high-frequency variations (on time scales < 2 hrs) are the dominant contributor to the short-term ionospheric variability. Such variations are often associated with traveling ionospheric disturbances with periods in the range of 40-80 mins. Analysis of anomalies (data-model differences) in ion temperature show significant correlation with high-latitude stratospheric planetary wave 1 amplitude, with positive correlation during daytime and negative correlation at night. We suggest that this correlation results from differences in gravity wave filtering by mesospheric zonal wind altered due to the influence of stratospheric planetary wave 1.

Keywords: ionosphere, mesosphere

Large-scale dynamics derived from a longitudinal chain of northern hemisphere SuperDARN radars

*Patrick J Espy^{1,2}, Robert E. Hibbins^{1,2}, Nora H. Stray^{1,2}, Robin Barnes³

1. Norwegian University of Science and Technology, Trondheim, Norway, 2. Birkeland Centre for Space Science, 3. Applied Physics Laboratory, The Johns Hopkins University

Although particular tidal and planetary wave modes are known to structure the ionosphere, wind observations from a single station produce a time-series from which only the total tidal harmonics can be detected. Similarly, long time-series from a single station can only give the net period and wind perturbation of the superposed spatial wavenumber components. While satellite data can give both temporal and spatial components, the time and spatial information is generally not separable without assuming stationarity. Here, hourly mean meteor wind data from a longitudinal chain of 8 mid-latitude northern hemisphere SuperDARN radars have been combined in order to provide the spatial tidal and planetary wave components as a function of time. This has been used to extract the migrating and non-migrating components of the semidiurnal tide, as well as the S1 and S2 planetary wave components in the lower thermosphere meridional wind between 1995 and 2016. Unlike in the southern hemisphere, the semidiurnal tide is dominated by the migrating (W2) component, though small but significant W1 and W3 contributions to the semidiurnal tide are measured, especially around the equinoxes. The large planetary wave amplitudes in the northern hemisphere can also couple into these tidal components. Data analysis and validation will be presented, together with initial results on the inter-annual variability of the tidal and planetary wave components and their possible coupling to the ionosphere.

Keywords: Dynamics, MLT, ionosphere

地磁気日変化から見積もられる電離圏電場の長期変動特性

Characteristics of long-term variations in the ionospheric electric field estimated with geomagnetic solar quiet daily variation

*新堀 淳樹¹、小山 幸信⁴、能勢 正仁²、堀 智昭³、大塚 雄一¹

*Atsuki Shinbori¹, Yukinobu Koyama⁴, Masahito Nose², Tomoaki Hori³, Yuichi Otsuka¹

1. 名古屋大学宇宙地球環境研究所、2. 京都大学大学院理学研究科附属地磁気世界資料解析センター、3. 東京大学大学院理学研究科地球惑星科学専攻、4. 大分工業高等専門学校

1. Institute for Space-Earth Environment Research (ISEE), Nagoya University, 2. Data Analysis Center for Geomagnetism and Space Magnetism Graduate School of Science, Kyoto University, 3. Department of Earth and Planetary Science, The University of Tokyo, 4. National Institute of Technology, Oita College

Geomagnetic solar quiet (Sq) variation observed on the ground is produced by the large-scale ionospheric currents flowing in the E-region of the ionosphere. The Sq currents are driven by the ionospheric electric fields consisting of polarization electric field and dynamo field ($V \times B$), where V and B indicates the neutral wind and background magnetic field, respectively. The neutral wind is driven by atmospheric tidal waves in the mesosphere and lower thermosphere (MLT) (60-150 km), which are caused by atmospheric heating due to solar extreme ultraviolet (EUV) radiation and an effect of atmospheric gravity waves. Therefore, to investigate the long-term variation in the ionospheric electric field estimated with the Sq variation is important to find the signals of long-term variation in the MLT and ionosphere. In this study, in order to clarify the seasonal and solar activity dependence of the ionospheric electric fields estimated with the Sq variation from 1958 to 2015, we analyze 1-hour geomagnetic field data obtained from 83 geomagnetic observatories from the middle-latitude to equatorial regions with an aid of the IUGONET data analysis tool. These geomagnetic field data were provided by WDC for Geomagnetism, Kyoto University. In this analysis, we first selected geomagnetic field data for the solar quiet days, which is defined as a day through which the Kp index is less than 4. Next, we identified the Sq variation as a deviation from the value at midnight in both the X and Y components of the geomagnetic field data. Finally, we obtained the monthly-mean ionospheric electric fields by solving Ohm's equation with the two-dimensional height-integrated ionospheric conductivity and geomagnetic Sq variation. As a result, the ionospheric zonal and meridional electric fields show a clear seasonal variation and 11-year solar activity dependence at all of the investigated geomagnetic stations. The power spectra of the zonal electric field show three dominant peaks in period at 6, 12 and 132 months. Moreover, the 4-month periodic component is also found in the middle-latitude region. The intensity of the zonal electric field is positively correlated with the F10.7 index near the equatorial region ($|q| < 20$ degrees, q : magnetic latitude) with no time lag, while they show a negative correlation in the middle-latitude region ($|q| > 20$ degrees). Such a latitudinal difference is seen in all the geographical longitudes. As a cause of the negative correlation in the middle latitudes, we infer that the neutral wind originating from solar tidal waves in the lower thermosphere weakens during a high solar activity due to the enhancement of ion drag effect.

キーワード：地磁気日変化、電離圏電場、季節変動、太陽活動、長期変動、IUGONET

Keywords: Geomagnetic solar quiet daily variation, Ionospheric electric field, Seasonal variation, Solar activity, Long-term variation, IUGONET

Dependence of ExB Drifts in the Night-Time Ionosphere on Winds and Conductivities

*Arthur D Richmond¹, Tzu-Wei Fang², Astrid Maute¹

1. NCAR, 2. U. Colorado

Plasma ExB convection in the night-time ionosphere is driven largely by the F-region dynamo, with additional effects due to boundary electric potentials at dawn and dusk and at high latitude. In the evening a vortex of convection over the magnetic equator is established, of which the upward branch represents the pre-reversal enhancement (PRE) of the vertical drift around 18-19 magnetic local time. The PRE affects the height of the ionosphere, the latitude distribution of electron density, and the likelihood of plasma instabilities. An approximate minimization principle for the night-time convection helps explain its dependence on the winds and conductivities. F-region winds in the Equatorial Ionization Anomaly region determine most of the electrodynamics of the entire low-latitude region at night. After sunset eastward winds drive plasma convection that increases toward the east, and normally causes plasma to be drawn up across lower-altitude geomagnetic-field lines to produce the PRE. Cowling conductivity in the night-time E-region equatorial electrojet retards the upflow, making the PRE sensitive to variable and poorly known night-time ionization.

An unseasonal equatorial plasma bubble event observed over Southeast Asia

*Brett A Carter¹, S. Tulasi Ram², E. Yizengaw³, R. Pradipta³, J. Retterer³, R. Norman¹, K. Groves³, R. Caton⁴, M. Terkildsen⁵, T. Yokoyama⁶, K. Zhang¹

1. RMIT University, 2. Indian Institute of Geomagnetism, 3. Boston College, 4. Air Force Research Laboratory, 5. Bureau of Meteorology, 6. National Institute of Information and Communications Technology

Recent progress has been made in describing the daily variability of Equatorial Plasma Bubble (EPB) occurrence using global physics-based thermosphere-ionosphere modeling, particularly during “peak” EPB seasons. Presented in this study is an analysis of an “off-peak” EPB event over the Southeast Asian region on the evening of 28 July 2014 that was not captured by the modeling performed in previous work.

Ground-based GPS scintillation, ionosonde and space-based GPS Radio Occultation (RO) data show the existence of Equatorial F-region Irregularities (EFIs) shortly after sunset over a region spanning 30° in longitude and 40° in latitude, centered on the geomagnetic equator. This EFI event was observed during a season when EPBs are expected to be rare/infrequent in the Southeast Asian longitude sector. Interestingly, GPS RO data indicates that this EFI event over Southeast Asia coincided with a suppression of EPBs in the African and Pacific longitude sectors, which were both experiencing a “peak” EPB season. Supporting ionosonde data reveals the presence of a strong pre-reversal enhancement (PRE) in the upward plasma drift over Southeast Asia on this day after sunset, and that this PRE was significantly stronger than on any other day of July 2014. An analysis of the geophysical conditions during this event reveals that this enhanced PRE was not caused by geomagnetic activity, and therefore was not due to storm-time penetration electric fields. Instead, it is suggested that forcing from lower altitudes, perhaps from tidal/planetary waves, could have caused this strong PRE. This strong PRE subsequently created favorable EPB growth conditions during an off-peak EPB season in the Southeast Asian sector, which manifested as unseasonal ionospheric scintillation activity across the region. The present inability to forecast such events is a significant and continuing challenge for ionospheric physics and space weather prediction.

Keywords: Equatorial Plasma Bubbles, Ionospheric Scintillation, Space Weather Forecasting, Thermosphere-ionosphere coupling

Spectral analysis of equatorial plasma bubbles obtained by high-resolution bubble model and C/NOFS satellite

Spectral analysis of equatorial plasma bubbles obtained by high-resolution bubble model and C/NOFS satellite

*横山 竜宏¹、Rino Charles²、Carrano Charles²、Groves Keith²、Roddy Patrick³

*Tatsuhiko Yokoyama¹, Charles L. Rino², Charles S. Carrano², Keith M. Groves², Patrick A. Roddy³

1. 情報通信研究機構、2. Institute for Scientific Research, Boston College, USA、3. Air Force Research Laboratory, USA

1. National Institute of Information and Communications Technology, Japan, 2. Institute for Scientific Research, Boston College, USA, 3. Air Force Research Laboratory, USA

Equatorial plasma bubbles (EPBs) are a well-known phenomenon in the equatorial ionospheric F region. As it causes severe scintillation in the amplitude and phase of radio signals, it is important to understand and forecast the occurrence of EPBs from the space weather point of view. EPBs are presently considered to evolve from the generalized Rayleigh-Taylor instability. It has been proposed that large-scale wave structure (LSWS) at the bottomside of the F region should be an important seeding of EPBs. However, it is quite difficult to observe the evolution of EPBs from a specific LSWS structure. Therefore, numerical modeling is a powerful tool to study the condition of EPB occurrence and day-to-day variability. In order to simulate the instability in the equatorial ionosphere, a three-dimensional high-resolution bubble (HIRB) model with a grid spacing of as small as 1 km was developed. Using the HIRB model, the nonlinear growth of EPBs from LSWS-like seeding, the formation of very turbulent internal structures such as bifurcation and pinching, and the east-west asymmetry of EPBs have been demonstrated.

A recent upgrade of the HIRB model has made it possible to conduct simulations with sub-kilometer grid spacing. Once EPBs penetrate into the topside ionosphere, turbulent internal structures become very significant. From the preliminary spectral analysis of higher-resolution simulation results, we obtain the power law characteristics of the turbulent structures of simulated EPBs. There are two power law components with a break point at around a few km wavelengths. The power law characteristics are consistent with past in situ observations such as the C/NOFS satellite to some extent. For more detailed analysis, wavelet-based analysis can be applied for the turbulent structures of the simulated EPBs, and the results can be compared with the same analysis applied for the C/NOFS satellite data. Such spectral information may be useful for the quantitative evaluation of radio wave scintillation intensity.

キーワード：赤道プラズマバブル、シミュレーション、C/NOFS

Keywords: equatorial plasma bubble, simulation, C/NOFS

Study of ionospheric irregularities in the 'temperate' mid-latitude region using the SuperDARN radars

*西谷 望¹、Ponomarenko Pasha^{2,1}

*Nozomu Nishitani¹, Pasha Ponomarenko^{2,1}

1. 名古屋大学宇宙地球環境研究所、2. サスカチュワン大学

1. Institute for Space-Earth Environmental Research, Nagoya University, 2. University of Saskatchewan

The Super Dual Auroral Radar Network (SuperDARN) is a network of HF radars deployed in the high and middle latitude regions of both hemispheres. Characteristics of ionospheric irregularities is one of the important topics which can be dealt with, using the SuperDARN. Since this network covers a wide latitudinal range, it can assess generation of ionospheric irregularities under an extended range of conditions. The Hokkaido Pair (HOP) of radars, located in the Northern Japan, are the only SuperDARN installations monitoring irregularities below 50 deg of geomagnetic latitude, the region often referred to as 'temperate' mid-latitude region. Here irregularities are commonly ascribed to the generation of polarization electric fields inside the Medium-Scale Traveling Ionospheric Disturbances (MSTIDs), whereas some of them are embedded in the steady convection structures unrelated to MSTIDs. In this paper we review SuperDARN studies of the ionospheric irregularities at the temperate mid-latitudes over the past 10 years as well as discuss future perspectives.

キーワード：電離圏不規則構造、SuperDARN、中緯度

Keywords: ionospheric irregularity, SuperDARN, mid-latitude

Impact of Midnight Thermosphere Dynamics on the Nighttime Middle- and Low-latitude Ionosphere

*Tzu-Wei Fang¹, Rashid Akmaev², YenChieh Lin³, Russell Stoneback⁴, Tim Fuller-Rowell¹

1. University of Colorado Boulder, USA, 2. NOAA Space Weather Prediction Center, USA, 3. National Central University, Taiwan, 4. University of Texas at Dallas, USA

Simulations using the coupled Whole Atmosphere Model and Global Ionosphere Plasmasphere Model (WAM/GIP) have successfully reproduced the unusual upward drift during the post-midnight period (~2-3 LT) that were observed by C/NOFS satellite during the recent solar minimum. Model produces significant day-to-day variability in the nighttime equatorial ionosphere and also reveals strong seasonal and longitudinal dependence of the nighttime upward drift. Our analysis indicates that the upward drifts are driven by thermosphere dynamics associated with the midnight temperature maximum (MTM). The MTM locally reverses the typical large-scale zonal and meridional wind pattern, in turn affecting the nighttime F-layer electrodynamics. The longitudinal variation of the drifts depends on the magnitude and position of the MTM peak relative to the magnetic equator. In this talk, we will present the morphology and characteristics of the post-midnight upward drift shown in the simulations and explain its causal mechanism. Additionally, simulation of growth rate of Rayleigh–Taylor instability associated with the nighttime upward drift and brightness waves produced by the MTM will also be discussed.

Keywords: Midnight Temperature Maximum, Low-latitude ionosphere, Equatorial Vertical Drift

Energetic particle impact on the Na layer

*津田 卓雄¹、高橋 透²、野澤 悟徳³、川原 琢也⁴、川端 哲也³、斎藤 徳人⁵、和田 智之⁵、Hall Chris⁶、小川 泰信²、細川 敬祐¹、中村 卓司²、江尻 省²、西山 尚典²、阿保 真⁷、津野 克彦⁵、Gumbel Jörg⁸、Hedin Jonas⁸

*Takuo T. Tsuda¹, Toru Takahashi², Satonori Nozawa³, Takuya D. Kawahara⁴, Tetsuya Kawabata³, Norihito Saito⁵, Satoshi Wada⁵, Chris M. Hall⁶, Yasunobu Ogawa², Keisuke Hosokawa¹, Takuji Nakamura², Mitsumu K. Ejiri², Takanori Nishiyama², Makoto Abo⁷, Katsuhiko Tsuno⁵, Jörg Gumbel⁸, Jonas Hedin⁸

1. 電気通信大学、2. 国立極地研究所、3. 名古屋大学、4. 信州大学、5. 理化学研究所、6. ノルウェー北極大学、7. 首都大学東京、8. スtockホルム大学

1. The University of Electro-Communications, 2. National Institute of Polar Research, 3. Nagoya University, 4. Shinshu University, 5. RIKEN, 6. The Arctic University of Norway, 7. Tokyo Metropolitan University, 8. Stockholm University

The metallic atom and ion layers, its source is considered as ablation of meteoroids coming into the atmosphere, are generally distributed mainly height range of 80-110 km or higher in the upper atmosphere. An importance of the metallic ions, such as Na⁺ and Fe⁺, is their longer chemical lifetimes, i.e. slower recombination rates, compared with major ions, such as NO⁺ and O₂⁺. This can contribute to maintain dens electron concentration, which can influence radio propagation in the upper atmosphere, e.g., satellite communication between the ground and space. The metallic atoms, such as Na and Fe, are also important as a reservoir of the metallic ions through their chemical processes. Thus, it is socially important to investigate the metallic atom and ion layers for understanding or prediction of the radio propagation environment in the upper atmosphere.

In this presentation, we will introduce our recent investigation, which focuses on energetic particle impact on the Na layer. There are several previous studies on this issue. Of interest is that the previous studies reported conflicting results and/or suggestions in the response of Na density to auroral activity. In some cases the Na density increased, and in others it decreased. Thus, the Na density response to auroral activity is still unclear. We have been working on this issue using ground-based observations, such as Na resonance scattering lidar and European incoherent scatter (EISCAT) radar, as well as Na dayglow measurements from space, such as Optical Spectrograph and InfraRed Imager System (OSIRIS) onboard the Odin satellite. As the results of our investigation, we conclude that the basic auroral effect to the Na density is a decrease not an increase and the decrease is probably induced through Na ion chemistry triggered by ionization due to energetic particle precipitation related with the auroral activity.

キーワード：Na層、高エネルギー降下粒子、オーロラ活動

Keywords: Na layer, energetic particle precipitation, auroral activity

Meteor radar observations at Mohe, China

*Libo Liu¹, Huixin Liu², Yiding Chen¹, Huijun Le¹, Yang-yi Sun²

1. Key Laboratory of Earth and Planetary Physics, Institute of Geology and Geophysics, Chinese Academy of Sciences,

2. Department of Earth and Planetary Science, Kyushu University

In this talk, we report the observations of the VHF all-sky meteor radar operated at Mohe (53.5 °N, 122.3° E), China, since August 2011. The kinetic temperature profiles retrieved from the observations of Sounding of the Atmosphere using Broadband Emission Radiometry (SABER) onboard the Thermosphere, Ionosphere, Mesosphere, Energetics, and Dynamics (TIMED) satellite are processed to provide the temperature (T_{SABER}) and temperature gradient (dT/dh) at 90 km height. Based on the SABER temperature profile data an empirical dT/dh model is developed for the Mohe latitude. First, a semiannual variation is dominated in the peak height of the height distribution of meteor echoes and there is an annual variation in the half width of the height distribution of meteor echoes. Secondly, we derive the temperatures from the meteor decay times (T_{meteor}) and the Mohe dT/dh model gives prior information of temperature gradients. Thirdly, the full-width of half maximum (FWHM) of the meteor height profiles is calculated and further used to deduce the temperatures (T_{FWHM}) based on the strong linear relationship between FWHM and T_{SABER} . The temperatures at 90 km deduced from the decay times (T_{meteor}) and from the meteor height distributions (T_{FWHM}) at Mohe are validated/calibrated with T_{SABER} . The temperatures present a considerable annual variation, being maximum in winter and minimum in summer. Harmonic analyses reveal that the temperatures have an annual variation consistent with T_{SABER} . Our work suggests that the FWHM has a good performance in routine estimation of the temperatures.

Acknowledgments

The TIMED/SABER kinetic temperature (version 2.0) data are provided by the SABER team through <http://saber.gats-inc.com/>. The temperatures from the NRLMSISE-00 model are calculated using Aerospace Blockset toolbox of MATLAB (2016a). This research was supported by National Natural Science Foundation of China (41231065, 41321003). We acknowledge the use of meteor radar data from the Chinese Meridian Project and from Data Center for Geophysics, Data Sharing Infrastructure of Earth System Science. The Mohe meteor radar was operated by Beijing National Observatory of Space Environment, Institute of Geology and Geophysics, Chinese Academy of Sciences.

Keywords: mesosphere, meteor radar

Response of diurnal tides to ENSO in the MLT region: a 21-year reanalysis GAIA model simulation result

*Liu Huixin¹, Sun Yang-Yi¹, Miyoshi Yasunobu¹, Jin Hidekatsu²

*Huixin Liu¹, Yang-Yi Sun¹, Yasunobu Miyoshi¹, Hidekatsu Jin²

1. 九州大学理学研究院地球惑星科学専攻、2. NICT

1. Dept. of Earth and Planetary Science, Kyushu University, 2. NICT

The whole atmosphere model GAIA is employed to investigate potential ENSO effect on the upper atmosphere. Driven by reanalysis data, effects of the strong El-Nino events in 1997-98 and 2015-2016 and La-Nina events during 1999 and 2010 are examined. Distinct features are revealed about ENSO impacts on tidal components 100 km altitude. 1. Tidal response to ENSO in meridional wind is different from those in Temperature and zonal wind 2. Tidal response in temperature and zonal wind show consistent features, with DW1 component enhances in autumn during El-nino events, DE2 and DE3 increases during La-Nina events. These characteristics provide us with a necessary global context to better connect and understand the upper atmosphere observations during ENSO events.

キーワード : tides、 ENSO、 vertical coupling

Keywords: tides, ENSO, vertical coupling

El Niño - Southern Oscillation effect on quasi-biennial oscillation of temperature diurnal tides in mesosphere and lower thermosphere

*Yang-Yi Sun¹, Huixin Liu¹, Yasunobu Miyoshi¹, Libo Liu², Loren Chang³

1. Kyushu Univsersuty, Department of Earth and Planetary Science, 2. Key Laboratory of Earth and Planetary Physics, Institute of Geology and Geophysics, Chinese Academy of Sciences, 3. Graduate Institute of Space Science, National Central University

The El Niño - Southern Oscillation (ENSO) is known as a periodic (2 to 7 years) planetary-scale ocean-atmosphere-coupled phenomenon that affects global climate and weather systems at various space and time frames. Studies in the recent decade suggested that the ENSO is a significant source of tides variability in the mesosphere and lower thermosphere (MLT). In this study, we examine the ENSO signals in the two dominant temperature diurnal tides of DW1 (diurnal westward wavenumber 1) and DE3 (diurnal eastward wavenumber 3) on the quasi-biennial oscillation (QBO) scale (18 to 34 months) in MLT. The tides are derived from the 21-year (1996 to 2016) GAIA (Ground-to-topside model of Atmosphere and Ionosphere for Aeronomy) temperature simulations and the 15-year (2002 to 2016) TIMED (Thermosphere Ionosphere Mesosphere Energetics and Dynamics) / SABER (Sounding of the Atmosphere using Broadband Emission Radiometry) temperature observations. The results show that the ENSO constrains the QBO not only in the stratosphere but also in the MLT. The anomalous stratospheric QBO in 2015–2016 enhances the DW1 in period from 1 to 1.5 years that is much shorter than the QBO period. The long-term decreasing trends in the DE3 QBO amplitude and the rainfall rate at low latitudes reveal the DE3 response to the climatological changes, of which the ENSO is one of the players.

Keywords: ENSO, QBO, diurnal tides

On the Relationship between Sporadic-E and ENSO Observed by FORMOSAT-3/COSMIC

Pei-Yun Chiu¹, *Loren Chang¹, Cornelius Csar Jude H. Salinas^{2,3}, Jann-Yenq Liu¹, Charles Lin⁴

1. Institute of Space Science, National Central University, Taiwan., 2. Taiwan International Graduate Program-Earth Systems Science, Academia Sinica, Taipei, Taiwan., 3. Department of Atmospheric Sciences, National Central University, Taoyuan City, Taiwan., 4. Department of Earth Science, National Cheng Kung University, Tainan, Taiwan.

Sporadic E (Es) refers to dense layers of metallic ions that can form in the ionospheric E region due to the effects of vertical neutral wind shear, influencing terrestrial and satellite radio propagation. The effects of Es can be observed by means of GPS scintillation in the E region, parametrized as the S4 phase fluctuation index. Here we present a report on the long term variation of Es using S4 indices and the zonal mean tropopause height measured by the FORMOSAT-3/COSMIC satellite constellation from 2007 - 2014. We find that the monthly global median S4 index in the E region shows a prominent dependence on variation of the El Nino-Southern Oscillation (ENSO) in the troposphere that has not been previously reported. The ENSO related variation of the E region global median S4 indices varies in phase with that of the zonal mean tropopause height, with both parameters lagging the Oceanic Nino index by four months. Taken together, these results indicate that ENSO signatures can be transmitted to Es formation mechanisms, potentially through modulation of the atmospheric waves and tides that alter lower thermospheric neutral wind shears by vertically propagating and breaking in that region.

Keywords: Sporadic E, ENSO, Tides

Meridional movement of northern and southern EIA in the East-Asia sector during 2002-2003 SSW

*Donghe Zhang¹, Xiaohua Mo², Larisa GONCHARENKO³, Shunrong Zhang³, Yongqiang Hao¹

1. Peking University, 2. Guangxi University for Nationalities, 3. Haystack Observatory, Massachusetts Institute of Technology

This presentation investigates the asymmetrical variability of the location of the north and the south equatorial ionization anomaly (EIA) crests in the East-Asian sector, along with their association with simultaneous observations of equatorial electrojet (EEJ) strength, geomagnetic activity index, and solar flux index during the 2002–2003 sudden stratospheric warming (SSW) event. Analysis of these observations indicates the existence of a large-scale quasi 16-day periodic meridional movement in both EIA crests, and also reveals a strong correlation between the quasi 16-day oscillation in geomagnetic latitudes of the EIA crest and EEJ strength. The latitude of the northern/southern EIA crest and the EEJ strength indicate that obvious synchronous periodic oscillations were in-phase in the northern and southern hemisphere when the SSW occurred. In addition, it is also found that both the EIA crest location and amplitude of the periodic movement of the EIA locations exhibit hemispheric asymmetry. The amplitude of the periodic movement of the EIA location in the southern hemisphere is larger than that of the northern hemisphere, and the southern EIA crest is further off from the equator than the north one. Understanding these asymmetries requires a combination of mechanisms that involve at least trans-equator meridional winds and the position of a sub-solar point; however, potential disturbances in neutral winds associated with the SSW may additionally complicate the equatorial ionospheric dynamics.

Keywords: equatorial ionization anomaly, sudden stratospheric warming, ionosphere

Vertical structures of stratospheric and mesospheric temperature changes during sudden stratospheric warming in northern high latitude

*Jeong Han Kim¹, Geonhwa Jee¹, Young-In Won², Back-Min Kim¹, Hae-Sun Choi¹, Seong-Joong Kim¹

1. KOPRI, Korea, 2. NASA/GSFC, USA

We analyze the temperatures obtained from Fourier Transform Spectrometer (FTS) and Micro Limb Sounder (MLS) onboard Aura satellite for two major SSW occurred in Jan. 2006 and Jan. 2009 in order to investigate the vertical structures of the stratospheric and mesospheric temperature changes with SSW phase. For our purpose, we divide wintertime into three periods and compute the height profiles of the correlation coefficients between daily MLS temperature anomalies of 45 height levels and about 33 km height, which can be thought to represent the stratospheric variability, using the mean value averaged over 65°N latitude. Our results showed that there seem to be a relatively weak and broad negative correlation between temperature anomaly at about 33 km height and temperature anomalies in mesosphere during pre-SSW, while this pattern seems to become stronger negative correlation during main phase. In addition, during the recovery phase, it seems to be shallower within the altitude range between about 40 and 80 km with strong positive correlation in the altitude range above about 80 km. We compare the results from observation with those from WACCM simulation and also investigate ozone variability in stratosphere during the recovery phase of major SSW. Preliminary results and some discussions will be presented.

Keywords: Stratospheric and mesospheric temperatures, Vertical profiles of correlation btw. stratosphere and mesosphere, Mesospheric cooling during SSW

Ionospheric E-region Plasma Irregularities Measured by Space Plasma Sensor Package Onboard Sounding Rocket IX

*Chi-Kuang Chao¹, Zai-Wun Lin¹, Ya-Chih Mao¹, Yen-Hsyang Chu¹, Ching-Lun Su¹, Shigeyuki Minami²

1. Graduate Institute of Space Science, National Central University, 2. Advanced Research Institute for Natural Science and Technology, Osaka City University

Space Plasma Sensor Package (SPSP) onboard Sounding Rocket IX was successfully launched from the south of Taiwan at 21:34 National Standard Time on 26 March 2014. It consists of a plasma impedance probe to measure electron density, a retarding potential analyzer (RPA) to measure ion temperature, an ion trap/ion drift meter/ion trap (IT/IDM) to measure ion currents and arrival angles, and a planar Langmuir probe to measure electron temperature. The RPA and IT/IDM are fabricated with high optical transparent electro-formed bonded gold meshes (100 LPI mesh density and 0.5 mil mesh thickness) in grid construction to minimize quasi-hysteresis effect. The two ion sensors are used as a pre-flight test of Advanced Ionospheric Probe for FORMOSAT-5 satellite scheduled to launch in 2017Q2. In the laboratory test, the current-voltage (I-V) curves measured by the SPSP indicate that PLP and RPA are almost free from contamination. In the flight test, all the sensors work well and meet design goals. During the up-leg path, nighttime E region is detected around 91-109 km altitude by IT/IDM and confirmed by the other sensors, RPA and PLP. An Es-layer is also found between 100 and 103 km altitude with peak at 101.6 km altitude. During the down-leg path, IT/IDM also detects the E region structure but cannot verify if the Es-layer exists due to weak current readings. It is noted that the preliminary geophysical parameters are derived without attitude calibration. The N_i , V_i , T_i , and T_e will be further calibrated according to attitude information from an onboard 3-axial fiber optical gyroscope and normalization on the I-V curves.

Keywords: Space Plasma Sensor Package, Sounding Rocket IX, Advanced Ionospheric Probe

Vertical velocity of acoustic wave detected with GNSS total electron content

*柿並 義宏¹、陳 佳宏²、劉 正彦³

*Yoshihiro Kakinami¹, Chia-Hung Chen², Jann-Yenq Liu³

1. 苫小牧工業高等専門学校、2. 台湾国立成功大学、3. 台湾国立中央大学

1. National Institute of Technology, Tomakomai College, 2. National Cheng Kung University, 3. National Central University

Acoustic waves are generated by the ground and sea surface motion after large earthquakes. The acoustic waves reach upper atmosphere and disturb plasma in the ionosphere through collision with neutral atmosphere. The ionospheric disturbance are observed ionospheric observation such as ionosonde and GNSS total electron content (TEC). Using dense GNSS network, the ionospheric disturbance associated with the earthquakes (co-seismic ionospheric disturbance, CID) has been investigated. Several type of traveling ionospheric disturbances are often observed. The one is associated with acoustic wave generated at the epicenter/tsunami source area. The velocity of the disturbance around 1 km/s. The other is associated with Ryle wave whose velocity is around 3 km/s. Further, localized ionospheric depletion (ionospheric hall) is observed after the earthquakes accompanied with tsunami. Since the center location of the ionospheric hall are located at the place of maximum vertical displacement, namely tsunami source area, it is concluded that the ionospheric hall is created by acoustic wave generated at the tsunami source area. Therefore, it is a quite plausible conclusion that the source of CID is generated at the maximum vertical displacement. Similar result is also obtained in the CIDs after Nepal earthquake occurred on 25 April 2015. The CIDs are mainly observed over the maximum vertical displacement located at east side of the epicenter. The result indicates that the conclusion is valid for not only submarine earthquake inducing tsunami but also inland earthquake. However, ambiguity of the location of the CID still exists because sub-ionospheric point is located at away from (close to) the sensor when the ionospheric layer is assumed at higher (lower) altitude. Therefore, the location of generation of acoustic wave has not been confirmed enough.

The CIDs are also observed after the foreshock of Tohoku earthquake occurred on 9 March 2011. In this case, initial point of CID were observed by using the signal of 3 GPS satellites. When estimation of the center of the CID is performed with triangulation using 3 satellites data, it is possible that accurate location of the center of the CID is estimated. Further, we found altitude difference of the estimated altitude of the disturbance from the results. From the result, vertical velocity of the acoustic wave is estimated at 1.03 km/s. These results suggest that using GNSS TEC is effective tool to estimate the location of maximum vertical displacement and vertical velocity of the acoustic wave.

キーワード：全電子数、音波、東北地震、地震後の電離圏擾乱、熱圏

Keywords: Total electron content, acoustic wave, Tohoku earthquake, co-seismic ionospheric disturbance, thermosphere

Evidence for Dynamical Coupling of Stratosphere-Mesosphere and Lower thermosphere (MLT) during 2010 minor Stratospheric Warming in Southern Hemisphere

*Eswaraiah Sunkara¹, Yongha Kim¹, Huixin Liu², Nicholas Ssessanga¹, Venkat Ratnam Madineni³

1. Dept. Astronomy and Space Science, College of Natural Sciences, Chungnam National University, Daejeon, 305-764, Korea, 2. Department of Earth and Planetary Science, Kyushu University, Fukuoka, Japan., 3. National Atmospheric Research Laboratory (NARL), Gadanki, Tirupati, India.

The coupling between stratosphere and mesosphere-lower thermosphere (MLT) was studied in the southern hemisphere (SH) during 2010 minor sudden stratospheric warmings (SSW). Three episodic SSWs were noticed from early August to late October in ECMWF data and the specified dynamics-Whole Atmosphere Community Climate Model (SD-WACCM) simulations. Utilizing wind data measured by a meteor radar at King Sejong Station (62.22°S, 58.78°W), we find that the mesospheric zonal winds at 82 km significantly differ from those of normal years due to enhanced planetary wave (PW) activity before the SSWs and secondary PWs in the mesosphere afterwards. The zonal winds in the mesosphere reversed approximately a week before the SSW occurrence in the stratosphere as has been observed in 2002 major SSW. The Ground-to-topside model of Atmosphere and Ionosphere for Aeronomy (GAIA) simulates similar zonal wind reversal that occurred in the lower thermosphere at 100-140 km two or three days before the associated SSW event. Since the periods of minor SSWs are characterized by low solar and geomagnetic activity, the observed and simulated variability in the MLT region is mainly due to SSW. We also find signatures of mesospheric cooling in association with SSWs using the Microwave Limb Sounder (MLS) measurements. However, according to the GAIA simulations, warming instead of cooling took place in the lower thermosphere around 120- 140 km after few days of SSW event. Thus, the observation and model simulation indicate for the first time that the minor SSW also affects dynamics of the MLT region over SH in the same way as the major SSW.

Keywords: Sudden Stratospheric Warming (SSW), Mesosphere and Lower Thermosphere, Meteor Radar, Stratosphere-MLT Coupling, GAIA simulations, MLT dynamics

北海道陸別観測所の大気光画像を用いた中間圏・電離圏波動の水平速度分布の長期統計解析

Long-term statistical analysis of horizontal phase velocity distribution of mesosphere and ionosphere waves in airglow images at Rikubetsu and Shigaraki, Japan

*土屋 智¹、塩川 和夫¹、竹生 大輝¹、藤波 初木¹、大塚 雄一¹、松田 貴嗣²、江尻 省²、中村 卓司²、山本 衛³

*satoshi tsuchiya¹, Kazuo Shiokawa¹, Daiki Takeo¹, Hatsuki Fujinami¹, Yuichi Otsuka¹, Takashi S. Matsuda², Mitsumu K. Ejiri², Takuji Nakamura², Mamoru Yamamoto³

1. 名古屋大学宇宙地球環境研究所、2. 国立極地研究所、3. 京都大学生存圏研究所

1. Institute for Space-Earth Environmental Research at Nagoya University, 2. National Institute of Polar Research, 3. Research Institute for Sustainable Humanosphere, Kyoto University

Atmospheric gravity waves (AGWs) transport momentum from the troposphere into the mesosphere and the thermosphere. The momentum deposit through wave breaking causes the large-scale pole-to-pole circulation. The vertical propagation of AGWs depends on the horizontal phase velocity. Thus, investigation of the horizontal phase-velocity characteristics of AGWs helps us to understand the dynamical variation of middle and upper atmosphere. On the other hand, the propagation direction of medium-scale traveling ionospheric disturbances (MSTIDs) seems to be different at different latitudes. However, the cause which determines their propagation direction has not been understood.

A new spectral analysis method has been developed to obtain power spectra in the horizontal phase velocity by using the 3-D FFT technique [Matsuda et al., JGR, 2014]. Takeo et al. (submitted to JGR, 2017) studied horizontal parameters of AGWs and MSTIDs over 16 years by using airglow images at wavelengths of 557.7 nm (emission altitude: 90-100 km) and 630.0-nm (200-300 km) obtained at Shigaraki, Japan (34.8N, 136.1E) which is located at the middle part of Japan.

In this study, we have applied the same spectral analysis technique to the 557.7-nm and 630.0-nm airglow images obtained at Rikubetsu, Japan (43.5N, 143.8E), which is at the northern edge of Japan, for 16 years from 1999 to 2014. We examined similarities and differences of horizontal wave spectra between Shigaraki and Rikubetsu over 16 years to see their dependence on locations.

The propagation direction of AGWs is northeastward in summer and southwestward in winter at both Shigaraki and Rikubetsu, but yearly variation of power spectral density is different between these two stations. In summer, the propagation direction of AGWs is northeastward irrespective of the phase velocity, probably due to wind filtering of these waves by the mesospheric jet. However, in winter, low phase-velocity waves (20-100 m/s) propagate to southwest, but high phase-velocity waves (100-150 m/s) propagate to southeast at both Shigaraki and Rikubetsu, suggesting reflection of westward high-velocity waves at both stations by the mesospheric jet. For MSTIDs, there is a negative correlation between yearly variation of powers spectral density and F10.7 flux at both sites. Propagation direction is southwestward in all season at both Shigaraki and Rikubetsu. The sub-peak at northeastward MSTIDs is larger in Rikubetsu than in Shigaraki. This may suggest latitudinal dependence of northeastward-moving MSTIDs, though further analysis will be needed for data at different stations.

キーワード：大気重力波、中規模伝搬性電離圏擾乱、スペクトル解析

Keywords: AGWs, MSTIDs, spectral analysis

Study of interannual gravity wave in the middle atmosphere over Syowa using Rayleigh/Raman lidar

*木暮 優^{1,2}、中村 卓司^{2,1}、江尻 省^{2,1}、西山 尚典^{2,1}、富川 喜弘^{2,1}、堤 雅基^{2,1}

*Masaru Kogure^{1,2}, Takuji Nakamura^{2,1}, Mitsumu K. Ejiri^{2,1}, Takanori Nishiyama^{2,1}, Yoshihiro Tomikawa^{2,1}, Masaki Tsutsumi^{2,1}

1. 総合研究大学院大学複合科学研究科、2. 国立極地研究所

1. The Graduate University for Advanced Studies, 2. National Institute of Polar Research

Gravity waves have important roles in transporting energy and momentum between the lower and upper atmosphere [Lindzen, 1981; Holton, 1982; Matsuno, 1982]. Their momentum deposition induces a meridional circulation from the summer pole to the winter pole, and the circulation makes the stratospheric temperature distribution in summer and winter away from radiative equilibrium. However, we have not completely known the quantification of gravity wave roles in the middle atmospheric circulation, especially Antarctic. A Rayleigh/Raman (RR) lidar was installed in January 2011 at Syowa Station, Antarctica (69°S, 40°E). The lidar has measured temperature profiles between 10 and 80 km since February 2011.

In this study, we investigated monthly mean gravity wave potential energy (Ep) in the height range of 15-70 km from May 2011 to October 2015 except for November, December and January. The number of nights used for this analysis is 360 nights in five years. Above 30 km altitude, Ep was maximized during winter in the each year. The seasonal dependence of Ep over Syowa was similar to Ep over Davis (69°S, 79°E) [Alexander et al., 2011; Kaifler et al., 2014] and McMurdo (78°S, 167°E) [Lu et al., 2015]. We also investigated the interannual variation of Ep in each year, and the variation was $\pm 40\%$. However, the Ep in August of 2014 was 3 times larger than that in August of the other years above 40 km altitude. We also compared the Ep with the location of the polar night jet according to Nash et al. [1996]. The comparison shows that the polar night jet existed over Syowa in August of 2014 and suggests that GWs from the polar vortex could contribute to Ep in August of 2014.

In this presentation, we will discuss the interannual variation of Ep and the contribution of the polar night jet.

キーワード：中層大気、ライダー、重力波、南極域

Keywords: middle atmosphere, lidar, gravity wave, Antarctic

Daytime ionospheric longitudinal gradients seen in the observations from a regional BeiDou GEO receiver network

*Fuqing Huang^{1,2}, Jiuhou Lei^{1,2}

1. School of Earth and Space Sciences, University of Science and Technology of China, 2. Mengcheng National Geophysical Observatory, University of Science and Technology of China

Many studies have devoted to the longitudinal variations of the ionosphere globally. However, the ionospheric longitudinal variations in a small region are rarely reported. In this paper, we use the TEC data from a BeiDou geostationary orbit (GEO) receiver network to investigate ionospheric longitudinal variations within the zonal scale of 1000 km in China. The BeiDou GEO TECs provide a good dataset to study longitudinal variations, compared with non-GEO TEC, without contaminating the spatial variations and elevation change due to satellite motion. Pronounced daytime longitudinal gradients within the distance of 1000 km are present in BeiDou GEO TEC observations. It was found that the TEC is larger in the west than in the east. In some cases, the TEC gradient magnitudes are larger than 20 TECU. For most events, the obvious daytime longitudinal gradients occurred under the weak and moderate geomagnetic activity conditions. In addition, daytime longitudinal gradients are mostly accompanied by TEC enhancement. We suggest that the observed daytime longitudinal gradients are probably associated with the electric field disturbances.

Keywords: ionospheric longitudinal gradients, BeiDou GEO TEC, small region, small region

Seasonal and spatial variation of He^+ column density in the evening topside ionosphere observed by ISS-IMAP/EUVI

*穂積 裕太¹、齊藤 昭則²、吉川 一朗³、山崎 敦⁴、村上 豪⁴、吉岡 和夫³

*Yuta Hozumi¹, Akinori Saito², Ichiro Yoshikawa³, Atsushi Yamazaki⁴, Go Murakami⁴, Kazuo Yoshioka³

1. 電気通信大学大学院、情報理工学研究科、2. 京都大学大学院、理学研究科、3. 東京大学、4. 宇宙航空研究開発機構 宇宙科学研究所

1. University of Electro-Communications, 2. Kyoto Univ., 3. The University of Tokyo, 4. Institute of Space and Astronautical Science / Japan Aerospace Exploration Agency

The seasonal, longitudinal and latitudinal variations of He^+ distribution in the evening topside ionosphere in 2013 - 2015 are elucidated with data of He^+ resonant scattering obtained by Extreme Ultra Violet Imager (EUVI) onboard the International Space Station (ISS). EUVI provides a data set of the column density of He^+ in the topside ionosphere. The data set provides a unique opportunity to study He^+ distribution in the topside ionosphere from a different perspective of past studies using in-situ measurement data. During the solstice seasons, an enhancement of He^+ column density in the winter hemisphere is observed. The magnitude of this hemispheric asymmetry shows a longitudinal variability. Around the June solstice, the hemispheric asymmetry was greater in the longitude sector where the geomagnetic declination angle is negative and smaller in the longitude sector where the geomagnetic declination angle is positive. Around the December solstice, on the other hand, this longitudinal variation of the asymmetry magnitude had opposite tendency. The hemispheric asymmetry of the effective neutral wind well explains this behavior of He^+ . The field-aligned component of neutral wind in the F-region is varied in longitude under the presence of finite geomagnetic declination angle and large zonal wind. We examined the seasonal and longitudinal variation of the effective wind with HWM14 model. In the equinox seasons, two longitudinal maxima were observed at around 140°E and 30°E. The longitudinal variation of the effective neutral wind is a candidate of these two maxima of He^+ concentration. These results suggest that the transport of ions in the topside ionosphere is strongly affected by the F-region neutral wind.

Fine Structure Interactions with Gravity Waves in the Mesosphere and Lower Thermosphere

*Tyler Mixa^{1,2}, David Fritts², Katrina Bossert², Brian Laughman², Ling Wang², Thomas Lund³, Lakshmi Kantha¹

1. University of Colorado Boulder, CO, USA, 2. GATS-inc Boulder, CO, USA, 3. NorthWest Research Associates Boulder, CO, USA

An anelastic numerical model is used to characterize the influences of fine layer structures on gravity wave propagation in the Mesosphere and Lower Thermosphere (MLT). Recent lidar observations identify persistent layering structures in the MLT that have sharp stratification and vertical scales below 1 km. Gravity waves propagating through finely layered environments can trigger the evolution of small scale instabilities that significantly enhance the layering in these regions. Such layers in turn promote ducting or reflection, hasten the onset of self-acceleration dynamics, encourage wave/mean-flow interactions, and filter the outgoing wave spectra, defining the wave's influence as it propagates to higher altitudes. Using high resolution simulations of a localized gravity wave packet in a deep atmosphere, we identify the impacts of various wave and mean flow parameters to determine the major mechanisms driving these dynamics and complement recent state-of-the-art observations.

Keywords: Gravity Wave, Wave Mean-Flow Interactions, Mesosphere and Lower Thermosphere

What Drives the Electrodynamics of the Low-Latitude Evening Ionosphere?

*Arthur D Richmond¹, William Evonosky², Tzu-Wei Fang³, Astrid Maute¹

1. NCAR, 2. U. South Florida, 3. U. Colorado

Neutral and plasma dynamics are strongly coupled in the F region. In the low-latitude evening ionosphere an eastward neutral wind is accelerated by a strong eastward horizontal pressure gradient force that is incompletely balanced by ion drag and viscosity. Plasma convection is driven mainly by the zonal neutral wind in the lower Equatorial Ionization Anomaly (EIA) region, balanced by ion-neutral collisions in the E and lower F regions. Increased night-time E-region conductivity retards both ion convection and neutral winds in the F region. Unless the E-region night-time conductivity is large, the accelerating eastward ion convection draws plasma up from lower apex heights, producing the equatorial F-region pre-reversal enhancement of vertical ion drift.

On the Relation between Sporadic-E and ENSO Observed by FORMOSAT-3/COSMIC

*Pei-yun Chiu¹, Loren Chang¹, Cornelius Csar Jude H. Salinas^{2,3}, Jann-Yenq Liu¹, Charles Lin⁴

1. Institute of Space Science, National Central University, 2. Taiwan International Graduate Program-Earth Systems Science, Academia Sinica, 3. Department of Atmospheric Sciences, National Central University, 4. Department of Earth Science, National Cheng Kung University

In recent years, many studies have shown evidence for several types of atmosphere-ionosphere coupling. In this study, we show the possible relation between Sporadic-E (Es) and El Nino-Southern Oscillation (ENSO) by using the FORMOSAT-3/COSMIC S4 scintillation index and tropopause height from 2007 to 2014. The long-term variation of the monthly global median S4 index in the E-region shows similar trend to ENSO, suggest that Es may be related to ENSO. The wavelet analysis may help us to verify the similar trend between scintillation and ENSO, but the mechanism of this coupling phenomenon still needs to be discussed and further explored.

Keywords: Sporadic E, ENSO, Tides

D-region oscillations of LF transmitter signals after the 2011 Off the Pacific Coast of Tohoku Earthquake

*大矢 浩代¹、瀧下 雄太、土屋 史紀²、品川 裕之³、野崎 憲朗、塩川 和夫⁴、中田 裕之¹、三好 由純⁴

*Hiroyo Ohya¹, Yuta Takishita, Fuminori Tsuchiya², Hiroyuki Shinagawa³, Kenro Nozaki, Kazuo Shiokawa⁴, Hiroyuki Nakata¹, Yoshizumi Miyoshi⁴

1. 千葉大学大学院工学研究科、2. 東北大学大学院理学研究科惑星プラズマ・大気研究センター、3. 国立研究開発法人情報通信研究機構、4. 名古屋大学宇宙地球環境研究所

1. Graduate School of Engineering, Chiba University, 2. Planetary Plasma and Atmospheric Research Center, Graduate School of Science, Tohoku University, 3. National Institute of Information and Communications Technology, 4. Institute for Space-Earth Environmental Research, Nagoya University

Although a lot of studies for the F-region ionosphere associated with earthquakes have been reported so far, few studies for the D-region ionosphere have reported. It is difficult to observe the D-region electron density by MF/HF radio sounding method such as ionosondes, because the MF radio waves are highly attenuated in daytime D-region, and HF radio waves penetrate into the D-region in both night and day. In this study, we investigate the D-region variations associated with the 2011 off the Pacific coast of Tohoku Earthquake (Magnitude 9.0) using intensity and phase of LF transmitter signals. The reflection height corresponds to electron density in the D-region. The propagation paths are Saga-Rikubetsu (RKB) over Japan and BPC (China)-RKB (Japan). As a result, there were two kinds of oscillations over both propagation paths after the mainshock: one was clear oscillations of the intensity with a period of about 100 s observed about 6 minutes after the mainshock, and the other was 30-90 s oscillations of the intensity and phase about 17 minutes after the mainshock. The one-to-one correspondence between the intensity and reflection height was not seen clearly. The changes of the intensity and reflection height for the oscillations were about 0.1 dB and 50 - 65 m, respectively. The time difference between the earthquake onset and the 100 s-oscillations was consistent with the propagation time of the Rayleigh waves (seismic waves) propagating from the epicenter to the LF propagation paths along the Earth surface, plus the propagation time of acoustic waves propagating from the ground to 68 km altitude vertically based on neutral atmosphere simulation. Thus, the LF oscillations may be caused by the acoustic waves excited by the Rayleigh waves. In the presentation, we will discuss the amount of change in the LF oscillations in more detail.

Ground-satellite conjugate observations of daytime traveling ionospheric disturbances by the GPS-TEC network and the CHAMP satellite over Japan: Preliminary results

*Aysegul Ceren Moral¹, Kazuo Shiokawa¹, Huixin Liu², Yuichi Otsuka¹, Michi Nishioka³, Takuya Tsugawa³

1. Institute for Space-Earth Environmental Research, Nagoya University, 2. Dept. of Earth and Planetary Science, Kyushu University, 3. National Institute of Information and Communications Technology

We report preliminary results of ground-satellite measurements of daytime traveling ionospheric disturbances (TIDs) over Japan by using the GEONET GPS receiver network and the CHAMP satellite. We use GPS measurements of TEC (Total Electron Content) and neutral and electron densities measured by CHAMP satellite for the years 2002 and 2008. A total of twenty-five TID events with ground-satellite conjugate measurements are found. On 2002, conjugate events are observed in January, 1 event, and February, 4 events. On 2008, twenty events are observed around winter months (January (3 events), February (5), March (1), October (3), November (5), and December (3)). For all events, there are clear southward moving structures in the GPS-TEC measurements. For all events neutral and electron densities measured by CHAMP show quasi-periodic fluctuations throughout the passages. The CHAMP satellite crossed at least one clear TID phase front for all the events. We observed corresponding phase relationships between total electron content (GPS-TEC) and neutral and electron densities measured by CHAMP. We categorized events into three categories; out-of-phase, in-phase and changing phase. In the presentation, we report correspondence of these TID structures seen in the ground TEC and CHAMP electron and neutral densities and discuss their phase relationship to identify the source of the daytime TIDs at middle latitudes.

Keywords: Daytime Traveling Ionospheric disturbances (TIDs) observed at mid-latitudes, Total Electron Content by using GPS satellite (GPS-TEC) and CHAMP satellite conjugate observations, TIDs caused by gravity waves in the neutral atmosphere

全球TECデータに基づく磁気嵐時の電離圏・プラズマ圏構造の時空間変動 Temporal and spatial variations of the ionosphere and plasmasphere during geomagnetic storms on the basis of global Total Electron Content (TEC) data analysis

*新堀 淳樹¹、大塚 雄一¹、津川 卓也²、西岡 未知²

*Atsuki Shinbori¹, Yuichi Otsuka¹, Takuya Tsugawa², Michi Nishioka²

1. 名古屋大学宇宙地球環境研究所、2. 情報通信研究機構

1. Institute for Space-Earth Environment Research (ISEE), Nagoya University, 2. National Institute of Information and Communications Technology (NICT)

It has been well-known that the global structures of the ionosphere and plasmasphere are drastically changed during the main and recovery phases of geomagnetic storms. These variations represent a complex response of the ionosphere-thermosphere-plasmasphere system to geomagnetic disturbances. Previous studies showed (1) a large enhancement of Total Electron Content (TEC) in the equatorial and middle-latitude regions within a few hours during a severe geomagnetic storm [e.g., Mannucci et al., 2005], (2) formation of storm-enhanced electron density (SED) extending from middle to high latitudes [e.g., Foster, 2013], and (3) physical process of SED formation and variation of the equatorial ionosphere on the basis of global SAMI3-Rice Convection Model (RCM) simulation [Huba and Sazykin, 2014]. However, these studies did not investigate detailed temporal and spatial variations of the ionosphere and plasmasphere with high time resolution during the main and recovery phases of geomagnetic storms using global TEC data. In this study, we clarify the temporal and spatial variations of the ionosphere and plasmasphere associated with development and decay of the geomagnetic storm occurred on October 11-12, 2010, on the basis of global TEC data obtained from Global Navigation Satellite System (GNSS) data. Moreover, we investigate the temporal and spatial variations of the plasmopause location from identification of ionospheric trough region from the latitudinal distribution of TEC. In this analysis, we used the geomagnetic Kp and SYM-H index and global TEC data, and the Inter-university Upper atmosphere Global Observation NETwork (IUGONET) data analysis tool [Tanaka et al., 2013]. These data are provided by World Data Center for Geomagnetism, Kyoto University, and Dense Regional And Worldwide International GNSS-TEC observation (DRAWING-TEC) project, NICT [Tsugawa et al., 2007], respectively. We first produced a global distribution of the 5-day quiet-time average TEC in a month of the investigated storm event. Here, we identified the 5 quiet days as a summation of the Kp index in each month. As a next step, we created a global map of difference of TEC (d-TEC) in between the storm-time and quiet-time periods, and investigated the global variation of the d-TEC during the main and recovery phases of the geomagnetic storm. During the pre-storm and initial phase of the geomagnetic storm, the d-TEC showed a small variation with the amplitude of less than 3 TECU for geographical latitude and longitude except for the equatorial and low-latitude (< 30 degrees, GMLAT: geomagnetic latitude). The spatial distribution of d-TEC did not almost change during this period. After the sudden commencement identified as a step-like increase of the SYM-H index, the d-TEC value began to increase in the middle-low latitudes (30-55 degrees) of the morning sector (9-10 h, LT: local time). As the geomagnetic storm is developed, the enhanced d-TEC region expanded to the afternoon sector (15 h, LT) within 4-5 hours. Moreover, 4 hours after the start of the main phase, the ionospheric trough region where the d-TEC value decreases significantly appeared in the afternoon sector (14-17 h, LT), and the location moved equatorward (67 to 54 degrees, GMLAT) associated with the development of the geomagnetic storm. This indicates that the plasmopause moves earthward in association with an intensification of convection

electric field. On the other hand, in the high-latitude region (> 60 degrees, GMLAT) of the morning sector (10-11 h, LT), a plume-like structure of d-TEC appeared, which corresponds to the SED phenomenon. The ionospheric trough and SED disappeared within 1 hour after the start of the recovery phase of the geomagnetic storm. The disappearance of these phenomena suggests that the SAPS/SAID activity and convection electric field decrease associated with the recovery phase of the geomagnetic storm.

キーワード：磁気嵐、全電子数 (TEC)、電離圏ープラズマ圏、電離圏電場、電離圏トラフ、プラズマ圏界面
Keywords: Geomagnetic storm, Total Electron Content (TEC), Ionosphere-Plasmasphere, Ionospheric electric field, Ionospheric trough, Plasmopause

SMILES-2 ミッション, 成層圏・中間圏・下部熱圏の衛星による観測計画 SMILES-2 mission, planned spaceborne observation of the stratosphere, mesosphere and lower thermosphere

*落合 啓¹、バロン フィリップ¹、入交 芳久¹、鵜澤 佳徳¹、西堀 俊幸²、鈴木 睦²、真鍋 武嗣³、前澤 裕之³、水野 亮⁴、長浜 智生⁴、塩谷 雅人⁵

*Satoshi Ochiai¹, Philippe Baron¹, Yoshihisa Irimajiri¹, Yoshinori Uzawa¹, Toshiyuki Nishibori², Makoto Suzuki², Takeshi Manabe³, Hiroyuki Maezawa³, Akira Mizuno⁴, Tomoo Nagahama⁴, Masato Shiotani⁵

1. 情報通信研究機構、2. 宇宙航空研究開発機構、3. 大阪府立大学、4. 名古屋大学、5. 京都大学

1. National Institute of Information and Communications Technology, 2. Japan Aerospace Exploration Agency, 3. Osaka Prefecture University, 4. Nagoya University, 5. Kyoto University

Spaceborne submillimeter-wave limb observation has a great advantage of measuring throughout the whole atmosphere from the stratosphere to the lower thermosphere with a single measurement technique. The variousness of atmospheric parameters to be observed, their precision, accuracy, and resolution are depends on the performance of submillimeter-wave receiver and antenna, which are the main components of submillimeter-wave limb sounding instrument, The SMILES-2 mission, which is a proposed spaceborne submillimeter-wave limb sounding mission proposed by our group, will be equipped with a highly-sensitive superconducting receiver and 1 m-class large aperture antennas. If the SMILES-2 mission is realized in full specifications, we expect the various observations to become possible. Temperature will be measured in a precision better than 1 K with a vertical resolution of 2-3 km in a height range between 15 and 80 km, in 5 K precision with 3-5 km vertical-resolution in a range between 80 and 120 km, and in 10 K precision with 10 km vertical-resolution in a range between 120 and 160 km. Wind will be measured in a precision better than 5 m/s with a vertical resolution of 2-3 km in a height range between 35 and 90 km, and in 10 m/s precision with 3-5 km resolution in a range between 90 and 160 km [Baron, 2015]. The frequency bands of the SMILES-2 receivers are selected to cover the emission lines from a variety of chemical species, which are important for the science in the stratosphere, mesosphere, and lower thermosphere. The species to be measured include O-atom, OH, O₂, O₃, H₂O, CO, NO, NO₂, N₂O, ClO, HCl, HOCl, OClO, BrO, HNO₃, CH₃CN, CH₃Cl [Suzuki, 2015].

The SMILES-2 receiver is a superconducting receiver. The spaceborne superconducting receiver was demonstrated in the successful international-space-station-borne mission, SMILES, in 2009. Comparing with 2 band receiver of SMILES at 624-626 GHz and 649-650 GHz, the SMILES-2 receiver will have many frequency bands, that is 485-489 GHz, 523-527 GHz, 556-558 GHz, 575-577 GHz, 619-627 GHz, 649-657 GHz, 1.8 THz and 2.06 THz. For THz band to observe OH and O-atom, a newly developed HEB mixer will be used. The main reflector of the SMILES-2 antenna will have about 1 m, which is made of CFRP with a reflection surface of aluminum. It is planned to have two antennas. Two antennas will see two directions, ahead and behind aslant, to observe an atmosphere twice from different directions so that the horizontal direction of wind is retrieved.

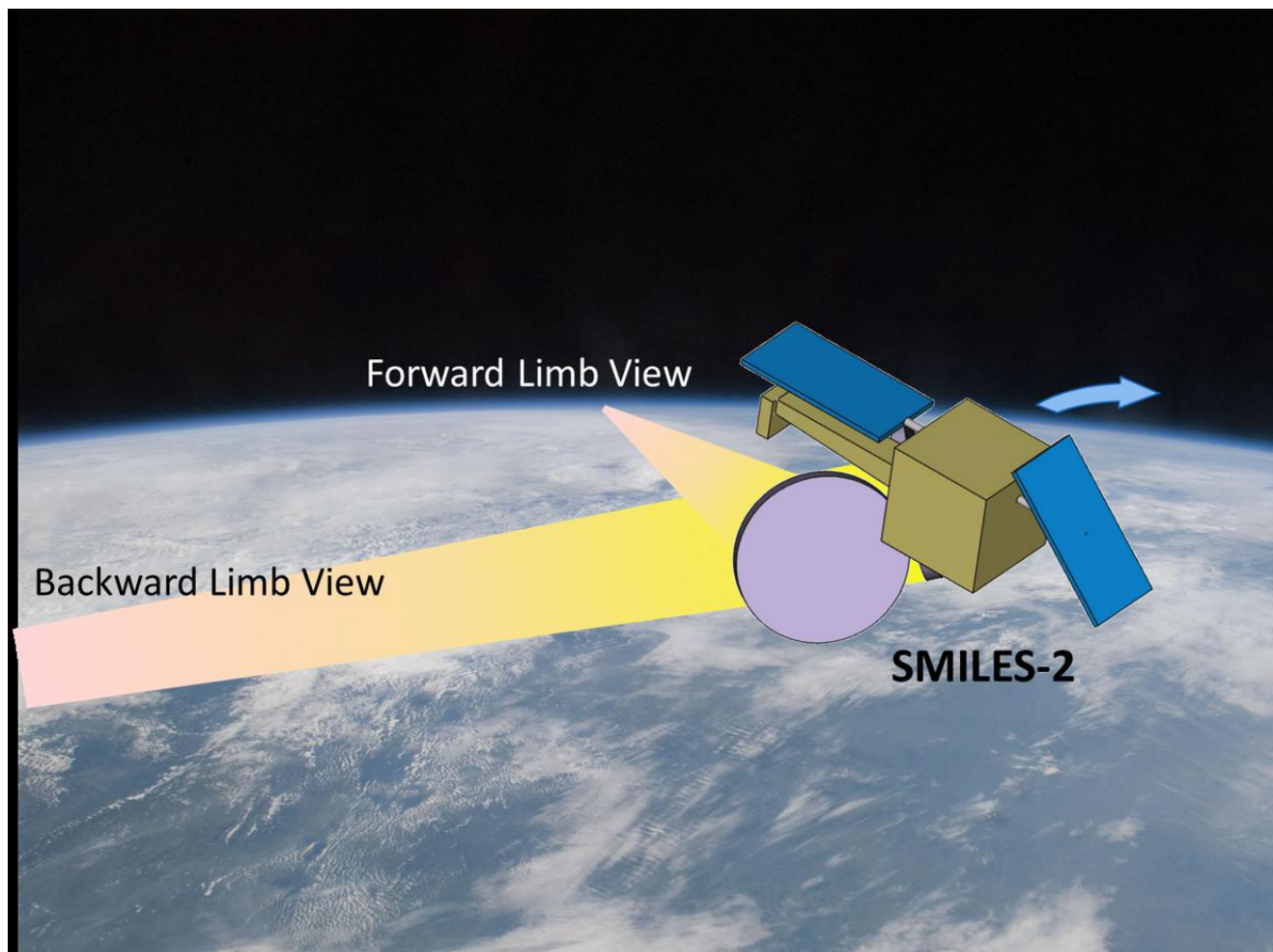
The satellite platform for SMILES-2 is assumed to be the JAXA small-size science satellite, whose weight can be about 700 kg. The satellite orbit is currently assumed to be a height of 550 km and an inclination of 66 degree. The conceptional design of the mission is now studied by SMILES-2 working group. The conceptional design of SMILES-2 will be compiled in the next year or later. If the proposal is selected by JAXA/ISAS, the mission may be launched in 2023 or later.

Baron et al. (2015), Proc. SPIE, 9639, doi: 10.1117/12.2194741.

Suzuki et al. (2015), Proc. SPIE, 9639, doi: 10.1117/12.2194832.

キーワード：衛星観測、中層大気、機器開発、サブミリ波、テラヘルツ、極低温

Keywords: satellite observation, middle atmosphere, instrument development, submillimeter wave, terahertz, cryogenic



Thermosphere response to doubling CO₂: simulation results with GAIA model

*中本 雄介¹、Liu Huixin¹、Miyoshi Yasunobu¹

*Yusuke Nakamoto¹, Huixin Liu¹, Yasunobu Miyoshi¹

1. 九州大学大学院理学府地球惑星科学専攻

1. Department of Earth and Planetary Sciences, Graduate School of Science, Kyushu University

Using the whole atmosphere model GAIA, we investigate the influence of doubling CO₂ on the thermosphere. Our results reveal consist cooling in the upper thermosphere as reported in previous work. Furthermore, we find that the cooling effect has distinct spatial and seasonal variation. First, it is stronger in polar regions than at lower latitudes. Second, it is stronger in local summer than in local winter. Third, it is stronger at night than at day. We investigate the mechanism for these variations by examining changes in the global circulation and composition.

キーワード : thermosphere、CO₂、vertical coupling

Keywords: thermosphere, CO₂, vertical coupling

Simulation of LF propagation modulation caused by earthquake by means of wave-hop method

*野崎 憲朗¹、品川 裕之¹、今村 國康¹、大矢 浩代²、土屋 史紀³

*Kenro Nozaki¹, Hiroyuki Shinagawa¹, Kuniyasu Imamura¹, Hiroyo Ohya², Fuminori Tsuchiya³

1. 国立研究開発法人・情報通信研究機構、2. 千葉大学、3. 東北大学

1. National Institute of Information and Communications Technology, 2. Chiba University, 3. Tohoku University

Fine observation of LF standard frequency and time signals (SFTS) at Rikubetsu, Hokkaido (RKB) detected oscillating structures on the received signal intensity and phase after 2011 Tohoku Earthquake. Electric field at the receiving point is described as vectorial summation of the electric fields due to the ground wave and sky waves. Numerical LF prediction by means of wave-hop method adopted in the Recommendation ITU-R P. 684-6 entitled “Prediction of field strength at frequencies below about 150 kHz” estimates the every component waves in the steady conditions. Only a few dominant mode contributes the total signal strength at the receiver. The electric field deviation of each component wave is obtained by fluctuating the reflection height of the ionospheric reflection point. A little uplift of the reflection height provides increased field strength of the component wave due to decreased ionospheric absorption. However, total electric field at the receiving point depends on phase relations between component waves. Receiving signal fluctuation is simulated as follows: 1. Calculate steady state condition parameters and synthesis all the component waves, then get the field strength at steady state. 2. Modulate each reflection height following to the earthquake perturbation spreading concentrically from epicenter. 3. Recalculate the propagation parameters of the component waves such as the SFTS propagation path length, ionosphere/ground incident angles, and absorption factors under the modified conditions. 4. Finally obtain the fluctuated field strength. Calculated field strength is consistent with the observation under the appropriate condition.

キーワード：長波伝搬、標準電波、波線法、地震波動

Keywords: LF radio wave propagation, Standard frequency and time signals, Wave hop method, Earthquake wave

Global features of ionospheric slab thickness derived from JPL TEC and COSMIC observations

*He Huang^{1,2}, Libo Liu^{1,2}

1. Key Laboratory of Earth and Planetary Physics, Institute of Geology and Geophysics, Chinese Academy of Sciences,
2. Beijing National Observatory of Space Environment, Institute of Geology and Geophysics, Chinese Academy of Sciences

The ionospheric equivalent slab thickness (EST), defined as the ratio of total electron content (TEC) to F2-layer peak electron density (NmF2), describing the thickness of the ionospheric profile. In this study, we retrieve EST from Jet Propulsion Laboratory (JPL) TEC data and NmF2 retrieved from Constellation Observing System for Meteorology, Ionosphere and Climate (COSMIC) ionospheric radio occultation data. The diurnal, seasonal and solar activity variations of global EST are analyzed. During solstices, daytime EST in the summer hemisphere is larger than that in the winter hemisphere, except in some high-latitude regions; and the reverse is true for the nighttime EST. The peaks of EST often appear at 0400 local time. The pre-sunrise enhancement in EST appears in all seasons, while the post-sunset enhancement in EST is not readily observed in equinox. The dependence of EST on solar activity is related to the inconsistent solar activity dependences of electron density at different altitudes. Furthermore, an interesting phenomenon is found that EST is enhanced from 0° to 120° E in longitude and 30° to 75° S in latitude during nighttime, just to the east of Weddell Sea Anomaly, during equinox and southern hemisphere summer.

Keywords: Slab thickness, Global features, COSMIC

Effect of Kelvin Waves on stratospheric QBO during *El Nino* periods using ECMWF reanalysis data

*Chen-Jeih Pan¹, Uma Das², Hsin-Chih Lai¹

1. Institute of Space Science, National Central University, 2. Department of Physics, Indian Institute of Information Technology Kalyani

35-year long dataset of temperature from ECMWF reanalysis has been analysed to obtain characteristics of Kelvin waves to understand the effect of El Nino Southern Oscillation (ENSO) on the Quasi Biennial Oscillation (QBO). Enhanced Kelvin wave activity is observed during El Nino periods when the phase of the QBO was easterly. Slow waves of wavenumber one and periods greater than 12 days are the most prominent Kelvin waves in the stratosphere during these periods, and showed significant wave-mean flow interactions. Comparison with outgoing longwave radiation (OLR) showed that there is increased convective activity over the Indonesian region and the East Pacific region during these periods of enhanced Kelvin wave activity. However, the rate at which the zero wind line preceding the westerly descended from 10 hPa to 50 hPa was not quite high, as was observed in the case of the 2009/2010 El Nino period. Careful examination showed that, instead of fixing the initial height at 10 hPa, if the slope of the zero wind line was calculated from the height at which the enhanced Kelvin wave activity interacted with the mean flow, the westerly did indeed descend very fast. Thus we conclude that during those El Nino periods when the QBO was easterly, the subsequent westerly showed an anomalous descent. This study emphasizes the importance of wave-mean flow interactions in maintaining the large scale circulation of the Earth's atmosphere.

Keywords: El Nino Southern Oscillation (ENSO), Quasi Biennial Oscillation (QBO)

Study on the Vertical Wavelength of the Atmospheric Kelvin Waves

*Hsin-Chih Lai¹, Chen-Jeih Pan²

1. Chang Jung Christian University, Taiwan, 2. National Central University, Taiwan

By using a length of 35-years old dataset of temperature from ECMWF re-analysis, the characteristics of the vertical wavelength of Kelvin waves to understand the effect of El Niño Southern Oscillation (ENSO) on the Quasi Biennial Oscillation (QBO) is analyzed. We concluded that the increased vertical wavelength could be the reason for the Kelvin wave not being able to interact with the mean flow. The observations indicated a clear modification in wave properties during the El Niño episode and emphasized the sensitivity of the atmospheric waves to various wave generation processes. An interesting event is the 12-day wave at wavenumber 1 whose vertical wavelength is approximately 10 km throughout the period of study and the phase lines do not 'see' the mean flow. The waves that do not interact with the mean flow must be traveling at higher altitudes. We also analyzed the temperature variation of upper atmospheric data to exam further details and the present study provides information regarding on the long-term morphology of the vertical wavelength.

Keywords: Kelvin Waves, ENSO/QBO, Long-term Morphology

Reverse Ray Tracing of Mesospheric Gravity Waves over the Antarctic Peninsula

*Brittany Williams¹, Eric Davis¹, Kim Nielsen¹, Michael Taylor²

1. Utah Valley University, 2. Utah State University

The majority of studies of atmospheric gravity waves are concerned with waves observed at equatorial and mid latitudes. In the early 2000' s Utah State University and British Antarctic Survey initiated a long term study of these waves over the Antarctica utilizing mesospheric airglow imagers, which has progressed into a comprehensive Antarctic observation network (ANGWIN). A recent long term analysis of gravity wave characteristics from two observation sites: Halley and Rothera, has revealed a distinct difference in predominate propagation directions between the two. Though Halley exhibited propagation directions changing with seasons, Rothera showed a remarkable fixed preference for westward propagating waves. While the waves observed over Rothera revealed freely propagating characteristics in the observed mesospheric region, their source location and origin remains unanswered. In this project we have focused on investigating the propagation of the waves from the observation point to their origin through a simple reverse ray tracing scheme. By analyzing ray tracing trends over two years of data we provide a preliminary overview of propagation characteristics and discuss the impact of orographic generated waves over the Antarctic peninsula.

Keywords: Aeronomy , Gravity Waves, Ray Tracing

Reverse Ray Tracing of Wintertime Mesospheric Gravity Waves Observed Over Interior Alaska

*Eric J Davis¹, Kim Nielsen¹, Michael Negale²

1. Utah Valley University, 2. Utah State University

While atmospheric gravity waves have been observed and studied in details for decades, there are still many questions to be addressed with respect to their propagation from the lower atmosphere into the mesopause region. Waves generated in the lower atmosphere are capable of transporting energy from their origin to the upper atmosphere as they propagate upward. While these energy transports have been known to impact large-scale circulation in the atmosphere, recent observations and model results have shown they also impact space weather and may play essential roles in climate changes. For the later, climate models often conclude at altitudes well below where we investigate the wave dynamics. New models increasing the top altitude have shown the importance of including the energy budget at these higher altitudes. Therefore, it has become increasingly important to characterize the wave propagation dynamics. A mesospheric airglow camera observed short-period gravity waves during the 2011-2014 winter months over interior Alaska. As an undergraduate research project we have developed a simple reverse ray tracing model to propagate the observed waves downward through the atmosphere to their respective points of origin. Here we present preliminary results of the reverse ray tracing algorithm and discuss propagation characteristics and possible source locations.

Keywords: Aeronomy, Gravity Waves, Ray Tracing

An automatical method for identification of polar cap boundary and patches by using in situ plasma measurements and its application

*Yu-Zhang Ma¹, Qing-He Zhang¹, Roderick Heelis², Zan-Yang Xing¹, Yong Wang¹

1. Shandong Provincial Key Laboratory of Optical Astronomy and Solar-Terrestrial Environment, Institute of Space Sciences, Shandong University, Weihai, 264209, China, 2. William B. Hanson Center for Space Sciences, University of Texas at Dallas, Richardson, Texas, USA

We have developed an automatical method to identify the polar cap boundary (PCB) and polar cap patches by using the in-situ plasma observations. Based on the difference of the typical source regions of the high-energy plasma, this method makes a double-Gaussian-like curve fitting to the integral energy flux with an energy range of 1392eV-30KeV for electrons and 4400eV-30KeV for ions, and then identifies the PCB by determining the poleward boundary of the regions where the energy flux are less than ± 1.5 times of the variance above the mean fluxes. Finally, we find the patch in the identified polar cap region by seeking the region where the plasma number density are more than twice larger than the average plasma density of the polar cap region. Applying this method, we automatic identified 15486 polar cap boundaries and more than 3000 patches from 2010-2014 passes of the polar region by the Defense Meteorological Satellite Program (DMSP) F16 and F17 satellites. We further differed dayside plasma blobs from patches by using the field-aligned current and precipitation energy flux observations, We Analyzing the in-situ plasma features inside these plasma irregularities and confirmed that rapidly moving patches are clear associated with ion upflow, and find the Poynting flux, associated with frictional heating, plays the dominated role for accelerating the ion upwelling at the center of polar cap region, while the field-aligned current, associated with electron heating, was mainly contributed to ion upflow in the dayside plasma blob.

Keywords: Identification of polar cap boundary from integral ion and electron energy fluxes, ionupflow associated with polar cap patch and dayside plasma blob

Neutral-ion coupling in the auroral ionosphere during magnetospheric substorms

*Lei Cai^{1,2}, Shin-ichiro Oyama², Anita Aikio², Heikki Vanhamaki², Ilkka Virtanen²

1. Ionospheric Physics Unit, Univ. of Oulu, Finland, 2. Institute for Space-Earth Environmental Research, Nagoya University, Japan

At high latitudes, the coupled ionosphere-thermosphere system is highly affected by interactions between the solar wind and the magnetosphere. The magnetospheric energy can be efficiently transferred into the ionosphere during magnetospheric substorms, via electromagnetic energy exchanges and auroral precipitation. Due to substorm energy input, ion-drag force and pressure gradient produced by Joule heating can become dominate forces that control the thermospheric wind. Although a few studies have shown that thermospheric dynamics can be strongly affected by auroral activities, it is still unclear that how the ion-neutral coupling process depends on different substorm phases. In addition, the variation of the thermospheric wind may be affected by the location of the substorm onset in respect to the observation site.

To investigate the questions above, we used measurements from 2009 to 2016 by ground-based instruments installed in northern Scandinavia, including European Incoherent Scatter (EISCAT) radars, Fabry-Perot Interferometer, all-sky cameras, and magnetometers. Those instruments provide an opportunity to measure several ionospheric and thermospheric key parameters such as plasma density, electric field, conductivities, equivalent currents, and the neutral wind. We studied the substorm evolution of thermospheric winds by analyzing individual events and by statistical methods. In the evening sector, the neutral wind has a typical westward acceleration during the substorm growth phase, mainly due to the strong ion-drag force associated with the equatorward motion of the enhanced eastward electrojet. The westward acceleration is terminated at a time close to substorm onset. During the expansion phase, the wind changes from westward to eastward. The transition time from westward to eastward depends on the longitudinal location of the onset. During the evolution, mesoscale disturbances were often observed, which are affected by the local auroral activity. We will discuss the physical mechanisms that cause the wind accelerations by analyzing the relative importance between ion-drag force and Joule heating.

Keywords: ionosphere-thermosphere coupling, substorm, neutral wind, equivalent current, auroral activity

Vertical and meridional propagations of 6.5DWs in stratosphere-MLT regions observed by satellite

*Yingying Huang¹, Huijun Li², Chongyin Li³, Shaodong Zhang⁴, Lingqi Zeng⁵

1. PLA University of Science and Technology, 2. Nanjing University of Aeronautics and Astronautics, 3. Institute of Atmospheric Physics, Chinese Academy of Sciences, 4. Wuhan University, 5. Institute of Geology and Geophysics, Chinese Academy of Sciences

6.5-day-waves (6.5DWs) are one of the most dominant planetary wave components in mesosphere and the lower thermosphere (MLT) regions, especially during equinoctial seasons. 6.5DWs amplitudes are almost tripled in the lower thermosphere than in stratosphere, and their seasonal variations are different. Are 6.5DWs in MLT propagated from stratosphere, or re-excited in MLT? In this paper, relationships between 6.5DWs in MLT and in stratosphere are analyzed. Firstly, vertical propagation characteristics of 6.5DWs in mid-high latitudes in both hemispheres during spring and autumn seasons are obtained, respectively, based on SABER/TIMED global observations from 2002 to 2016. Then results in the Northern Hemisphere (NH) and the Southern Hemisphere (SH) are compared to obtain inter-hemispheric similarities and discrepancies. Given these results and by utilizing wind data observed by TIDI/TIMED as well, wave-flow interactions through vertical propagations of 6.5DWs are analyzed. We first obtain results from case study, and then draw general conclusions from statistics researches. Previous studies have inferred that 6.5DWs could probably propagate along meridional directions [Liu, et al., 2004, Belova, et al., 2008]. It has been showed that 6.5DWs in MLT regions of one hemisphere may be propagated from stratosphere of the other hemisphere, and their amplitudes could be strengthened in unstable regions along their paths. However, these suggestions need to be proved by more observation evidences. The second part of this paper discusses possible meridional propagations of 6.5DWs based on SABER/TIMED and TIDI/TIMED observations. Results obtained in this paper could be useful in improvement of future atmospheric models of stratosphere-MLT regions.

References

- Liu, H.-L., E. R. Talaat, R. G. Roble, R. S. Lieberman, D. M. Riggin, and J.-H. Yee (2004), The 6.5-day wave and its seasonal variability in the middle and upper atmosphere, *J. Geophys. Res.*, 109, D21112, doi:10.1029/2004JD004795.
- Belova, A., S. Kirkwood, D. Murtagh, N. Mitchell, W. Singer, and W. Hocking (2008), Five-day planetary waves in the middle atmosphere from Odin satellite data and ground-based instruments in Northern Hemisphere summer 2003, 2004, 2005 and 2007, *Ann. Geophys.*, 26, 3557–3570.

Keywords: stratosphere-MLT, planetary waves, satellite observations

Characteristics of travelling ionospheric disturbances observed by Kharkiv and Millstone Hill radars

*Larisa Goncharenko¹, Sergii Panasenko², Philip Erickson¹, Igor Dominin²

1. Massachusetts Institute of Technology, Haystack Observatory, USA, 2. Institute of Ionosphere, Kharkiv, Ukraine

Travelling ionospheric disturbances (TIDs) represent a key dynamic process of energy transfer in horizontal and vertical directions, and one of the important sources of ionospheric variability. Acoustic gravity waves (AGWs) play a key role in coupling of different atmospheric regions through momentum and energy transfer, and TIDs are thought to be the manifestations of AGWs at ionospheric heights. The incoherent scatter method is well suited for TID studies as it enables TIDs detection in multiple ionospheric parameters (electron density, ion and electron temperatures, plasma velocity), and thus provides critical information needed to examine different hypothesis about association of TIDs with their sources.

In 2016, two coordinated measuring campaigns have been held near the vernal equinox and summer solstice using Kharkiv (49.6 N, 36.4 E) and Millstone Hill (42.6 N, 288.5 E) IS radars. The goal of joint observations was to detect TIDs and estimate their characteristics during these geophysical periods as well as to find similarities and differences in results obtained at various longitudes.

During the vernal equinox, the prevailing TIDs are observed near the sunrise and sunset solar terminators by both Kharkiv and Millstone Hill. The TID periods generally fall within the ranges of 40 –80 mins and 20 –40 mins. Relative TID amplitudes over Kharkiv are usually 3–15% and 2–10% of background electron density and plasma temperatures, respectively. At Millstone Hill, these values are greater and reach 10–35% for TIDs in electron density and 5–15% for TIDs in electron and ion temperatures. Larger values of TIDs amplitudes over Millstone Hill may indicate the longitudinal differences.

As for summer solstice, the overall wave activity was weaker. Despite the absence of solar terminators over Kharkiv at the heights above 250 km, TIDs occurred near the periods of terminator passage at lower heights. These results confirm the hypothesis that observed TIDs are caused by AGWs generated in the middle and lower atmosphere and propagating upward. The TIDs over Millstone Hill are mainly observed around solar terminator periods, similarly to the vernal equinox. Prevailing periods for TIDs over Kharkiv and Millstone Hill are of 40 –80 and 20 –40 mins. The values of relative amplitudes over Kharkiv are 8–20% and 3–8% of background electron density and plasma temperatures, respectively. These values are similar for Millstone Hill.

Conducting systematic long-term observations of wave processes in the ionosphere using all facilities available at Kharkiv and Millstone Hill observatories will enable to reveal longitudinal variability in TID characteristics, provide a better understanding of the mechanisms of TID generation and propagation, and improve regional and global ionospheric models.

Keywords: traveling ionospheric disturbances, gravity waves

A simulation study of seasonal variations in the thermospheric upward propagation of migrating terdiurnal tide

*Haibing Ruan¹, Jiuhou Lei¹

1. University of Science and Technology of China

The migrating terdiurnal tide in the mesosphere and lower thermosphere (MLT) is suggested to contribute significantly to the formation of the Midnight Temperature/Density Maximum (MTM/MDM) in the upper thermosphere. In this study, the Thermosphere Ionosphere Electrodynamics Global Circulation Model (TIEGCM) and the extended Canadian Middle Atmosphere Model (eCMAM) are utilized to investigate the seasonal variations of the upward propagation of the migrating terdiurnal tide from the MLT. Three main conclusions are drawn from a series of controlled simulations: 1) The background thermospheric zonal and meridional winds and neutral temperature can affect the upward propagation of the terdiurnal tide. 2) The background zonal winds can play an important role in the variation of the vertical advection and adiabatic cooling/heating, especially in the low thermosphere, and as a consequence, the upward propagation of the terdiurnal tide is modulated. 3) The terdiurnal tide in the MLT influences not only on the latitudinal distributions and magnitudes of the terdiurnal tide in the upper thermosphere, but also on the effect of the background winds on the upward propagation of the terdiurnal tide.

Keywords: Terdiurnal tide, Upward propagation, Seasonal variation